

Parallel determination of phenotypic cytotoxicity with a micropattern of mutant cell lines

Ryan S. Sincic · David A. Chang-Yen · Mark Eddings ·
Louis R. Barrows · Bruce K. Gale

© Springer Science + Business Media, LLC 2008

Abstract This work presents a novel tool, the Continuous Flow Microspotter (CFM) and its use in patterning cellular microarrays of multiple cell types into the bottom of a tissue culture well. The CFM uses a system of isolated microfluidic channels to make an array of localized microspots of adhesion dependent cells in the bottom of a conventional tissue culture well. With this device we have created micropatterns of multiple cell lines in a single tissue culture well and used this system to conduct simultaneous cytotoxicity tests and recover dose survival curves in a parallel study. This mechanism of parallel testing allows the researcher to employ the use of positive and negative controls, as well as compare the chemical response of phenotypes in a tightly controlled microenvironment. For the experiments presented in this paper we have fabricated a CFM with a set of ten microchannels (five inlet channels

and five outlet channels) to pattern a row of five microspots consisting of four cellular microspots and one empty spot for background measurements. Micropatterns containing a set of four different Chinese hamster ovarian cell (CHO) mutant phenotypes were deposited into the bottom of commercially available tissue culture wells then interrogated with mitomycin C, a chemotherapeutic agent. This study shows statistically significant ($P < 0.05$) hypersensitivity of the UV20 CHO mutant to a DNA interstrand cross-linking agent (mitomycin C). Because the CFM is also capable of depositing proteins and other biomolecules to the individual microspots of the array we foresee capabilities of the 48 microspot CFM to multiplex 48 cell types with 48 chemical reagents all within the confines of a 60 mm² area.

Keywords Cell patterning · Micro-array · Bioassay · Pharmacology · Toxicology · MEMS

Abbreviations

CFM continuous flow microspotter
CHO chinese hamster ovarian cell
NA numerical aperture
PDMS polydimethylsiloxane

R. S. Sincic (✉)
Department of Biomedical Engineering, University of Utah,
50 S. Central Campus Dr., Rm. 2480 MEB,
Salt Lake City, UT 84112-9202, USA
e-mail: sincic@gmail.com

D. A. Chang-Yen
Department of Biomedical Engineering, University of Utah,
50 S Central Campus Drive Rm 2110,
Salt Lake City, UT 84112, USA

M. Eddings · B. K. Gale
Department of Mechanical Engineering, University of Utah,
50 S Central Campus Drive Rm 2110,
Salt Lake City, UT 84112, USA

L. R. Barrows
Department of Pharmacology and Toxicology, University of Utah,
30 S. 2000 E., Rm 201,
Salt Lake City, UT 84112, USA

1 Introduction

Experiments to study cellular behavior are often conducted using chemical interrogation. These experiments require homogeneity in chemical dilution among other environmental controls. For the purpose of many cellular experiments tissue culture well plates have become a standard for maintaining environmental control, adding chemical reagents, tracking cell types and experimental variables. If

experiments could be conducted on a large, diverse number of cell types simultaneously in a single tissue culture well rather than across multiple wells, we could increase the homogeneity as well as degree of control within the environment and chemistry of the cellular experiment. Conducting a large number of cellular experiments in a single tissue culture well would also reduce the amount of reagents and materials used. For these purposes we have developed a device, the Continuous Flow Microspotter (CFM), for patterning microarrays of multiple cell types into the small uniform environment of a single tissue culture well.

This paper presents a set of experiments using the CFM to pattern a set of microspots containing multiple cell types within a single tissue culture well. We have used this cellular microarray to conduct a parallel test for phenotypic chemical–cell interaction. Built into these experiments is a bioassay containing positive and negative controls all within the same cellular array and tissue culture well. This strategy uses arrays of parallel microfluidic channels (Chiu et al. 2000a) for depositing and patterning a selection of mutant cell lines lacking a set of DNA repair mechanisms: base excision repair (Taverna et al. 2003; Brem and J. Hall 2005), non-homologous recombination (Kemp and Jeggo 1986; Cortez et al. 1999) and nucleotide excision repair (Gaillard and Wood 2001). These cell lines mimic cancer cells in that they lack mechanisms for DNA damage repair that are normally present in their healthy non-mutated homologues. DNA repair deficiencies can be used as targets for chemotherapy agents making it desirable to identify mechanisms of toxicity and phenotypic drug sensitivity. Because testing chemicals against a great number of phenotypes requires an extensive amount of chemicals and reagents, some of which may be expensive or rare, methods to reduce reagent usage, including miniaturization of these tests, are being developed.

Micropatterns of cells have been created using a variety of techniques (Flaim et al. 2005; Lee et al. 2005; Suh et al. 2004; Vogt et al. 2005; Cheng et al. 2004; Goto et al. 2007). Most commonly researchers will pattern ECM proteins to create an adhesive template for cells. Other groups have addressed the problem of adhering cells in micropatterns by performing complex surface modifications such as thermal activation (Cheng et al. 2004) and electroactivation (Yousaf et al. 2001) of substrates. These surface modifications increase expense and are not always ideal for cell viability and imaging. Most of these techniques are limited to depositing one cell type per pattern. Among the few techniques that have been demonstrated for patterning multiple cell types (Chiu et al. 2000b; Xu 2002) are methods that include the use of microfluidic channels (Chiu et al. 2000a, b). The CFM has been designed to adhere cells to surfaces treated with ECM proteins, similarly to the previously used methods.

In order to perform microscale parallel bioassays, researchers have patterned test agents, such as cDNA and other biomolecules on surfaces (Ziauddin and Sabatini 2001; Flaim et al. 2005), before depositing monolayers of cells which were influenced by the variations in the underlying substrate. These techniques only allow for testing one cellular phenotype per assay. It has been suggested that tools are necessary for creating patterns of multiple cell lines in order to determine whole cell responses manifested by different phenotypes (Xu 2002).

To meet these needs, we have developed a microfluidic tool for parallel deposition of multiple cell types into commercially available tissue culture well plates (Fig. 1). For the experiments presented in this paper we have fabricated a CFM with a set of ten microchannels (five inlet channels and five outlet channels) to pattern a row of five microspots consisting of four cellular microspots and one empty, control spot for background measurements. The primary advantage of our system compared to other cell patterning techniques (Flaim et al. 2005; Lee et al. 2005;

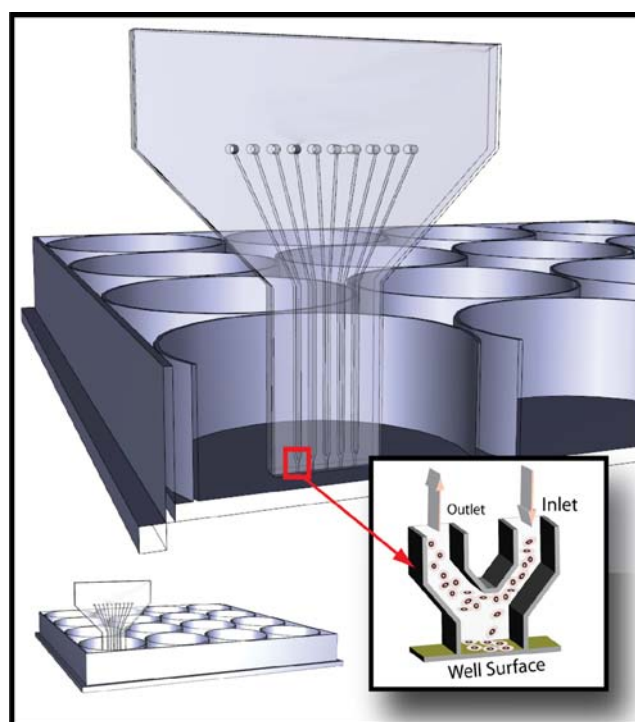


Fig. 1 Overview of the microfluidic cell patterning device. The CFM is shown contacting the well bottom (16 mm diameter). Parallel sets of microchannels run perpendicular to the well bottom for 30 mm to clear the height of the well (17 mm), at which point the channels diverge to allow for adequate space to interface with microtubing. The area of the well surface isolated by the deposition chamber is $200\ \mu\text{m} \times 300\ \mu\text{m}$ to pattern a proportionate cellular microspot. The CFM shown in this image will pattern up to five microspots. Similar PDMS microchannel layers can be bonded to the face of the one shown to create arrays with multiple rows. Not shown in this figure are the manifold used to position the CFM within the well and microtubing to interface fluids with the microchannel

Suh et al. 2004; Vogt et al. 2005; Cheng et al. 2004; Goto et al. 2007) is that each cellular microspot of our array is addressed by an independent pair of microfluidic channels. This independent addressing allows for cells and materials to be directed uniquely to every spot of the array, so each spot of cells essentially becomes an independent experiment. Alternatively, the entire pattern of cells can be subjected to the homogeneous environment of a 100 μL well. Maintaining this level of control in comparison studies of cell lines gives the researcher tools for experiments where homogeneity and control are essential.

Currently many cell studies are performed using transparent, tissue culture treated well plates that are purchased with their internal surfaces coated with cellular nutrients. The use of these well plates facilitates cell viability, cell imaging, and the chemical treatment of cells. Therefore, we found it a logical continuance of current practice to adapt our device to patterning cells in the tissue culture well plates common in biology labs. Until now we have not seen cell micropatterning tools that pattern cells into tissue culture wells. This may be due to the high aspect ratio (depth) of the wells. Still, researchers have indicated a need to fabricate cell arrays on substrates that are transparent, flexible, small and well contained (Xu 2002).

We believe that direct localization of cells using microfluidic channels onto a tissue culture treated substrate is a simple and direct approach to cell patterning. We have found that micropatterning cells in commercially-available, treated tissue culture wells provides a platform for convenient cell array maintenance, chemical delivery, and fluorescent imaging, where cellular arrays can be treated with volumes of <100 μL .

In order to demonstrate the utility of this microfluidic cell deposition system for parallel chemical tests on multiple cell phenotypes, we have demonstrated simultaneous deposition and patterning of four Chinese hamster ovarian (CHO) mutant cell lines, three with specific defects in particular DNA repair mechanisms: EM9 cells defective in repair of single strand DNA breaks (Barrows et al. 1998), XRS-6 cells deficient in DNA double-strand break repair (Zhou and Povirik 2005), UV20 cells deficient in DNA nucleotide excision repair (Moynahan et al. 2001), and the AA8 CHO wild type. This study reveals that the UV20 CHO phenotype is hypersensitive to mitomycin C (a DNA interstrand cross-linking agent) by parallel determination of dose survival response and by showing statistically significant ($P < 0.05$) phenotypic sensitivity

2 Materials and methods

Fabrication of microfluidic cell deposition device The microfluidic deposition device (the Continuous Flow

Microspotter, CFM) is fabricated by stacking layers of poly(dimethylsiloxane) (PDMS) microchannels to create a three-dimensional channel system for patterning two-dimensional arrays of cellular or protein microspots, with each spot addressed by a pair of microfluidic channels as illustrated in Fig. 1. The CFM is designed to pattern up to 48 microspots of proteins in 4×12 arrays addressed by 96 microchannels (48 pairs), adapted to a 96 well fluid manifold. For the purposes of this study, a two-layer prototype for patterning a single row of five microspots instead of the full 48 spot array was used. Patterning a reduced number of microspots facilitated tracking of inter-spot and inter-channel crosstalk, as well as background cell growth. Each of the five microspots in the pattern was addressed by an inlet and outlet channel as shown in Fig. 1.

Fabrication of a two-layer CFM involves five steps, (a) fabrication of the SU-8 positive relief mold for forming PDMS microchannels, (b) formation of PDMS layers containing microchannels and formation of PDMS layer for channel lid and support, (c) coring holes at the inlets and outlets of the microchannels, (d) bonding PDMS channel layers and lid layer, and (e) making a vertical planar cut across the microchannels to form the deposition chamber and to provide the area of fluid contact with the substrate.

SU-8 molds were fabricated on silicon wafers using conventional UV photolithography techniques (Chang-yen et al. 2006). UV dark field masks for generating microchannel patterns on negative photoresist were fabricated using a sign cutter (Graptect) to cut UV transparent regions of the mask out of a UV opaque material (Rubylith 100, Ulano Corp). The masking pattern is first created in Adobe Illustrator (Adobe Systems Incorporated) and transferred to the sign cutter via a USB connection with a laptop computer. The sign cutter cuts the pattern into the Rubylith with the precision necessary to generate <10 μm features (Bartholomeusz et al. 2005). Once the pattern outline had been cut out by the sign cutter, microchannel regions were then pulled away from the mask leaving transparent windows defining the shapes of the channels.

The structure of the device includes a layer (or multiple layers) of PDMS channels and a sealing lid layer for enclosing channels and structural support (Fig. 1). Channel layers were fabricated by molding PDMS on the SU8 mold made in step (a). A coring tool was used to puncture 1/16 in. holes through the inlet and outlet interfaces of the microchannels where 1/16 in. tubing (Upchurch) seals upon insertion. Immediately after the coring process a layer of uncured PDMS is spread across the lid layer and wiped with a razor leaving a thin residue of PDMS on the surface. The microchannel side of the channels layer was then placed in contact with the residue side of the lid and cured at 65°C for 45 min to cross-link the PDMS residue

and bond the two layers. This method of bonding can also be used to stack additional channel layers one over the next to produce the two-dimensional arrays of microchannels. After bonding, a razor blade was used to make a vertical planar cut along the bottom of the deposition chamber to provide the area of fluid contact between the microchannel and substrate. A micromanipulator was built to clamp the CFM over the surface being patterned. The micromanipulator used a thumb screw to control the contact pressure between the CFM and target substrate, allowing a liquid seal to be formed between the bottom of a cell culture well and CFM tip.

Cell cultures CHO cells (American Type Cell Culture) were cultured in α -MEM (HyClone, Logan, UT) supplemented with 10% fetal bovine serum (Summit, Ft Collins, CO), 250 ng/mL Fungisome (Biowhittaker, Walkersville MD), 100 μ g/mL streptomycin and 100 units/mL penicillin (Hyclone). The cell cultures were maintained at 37°C in a humidified atmosphere containing 5% CO₂. Before patterning in the cell culture wells, cells were washed and dissociated from culture plates with trypsin/EDTA (GIBCO), washed with α -MEM and resuspended in the cell culture medium at a concentration of $\approx 10^6$ cells/mL. All cells were cultured using the same conditions and medium.

Cell patterning Cellular micropatterns were printed into 16 mm diameter flat bottom tissue culture treated polystyrene wells (Corning Glass Works, NY). To pattern cells we used the following process steps; (a) filled the microchannels with culture medium to clear the air from the system, (b) lowered the CFM deposition chambers over pre-positioned alignment marks on the underside of the well clamping the contact surface of the CFM to the well bottom, (c) pumped more culture medium through the microchannel to ensure a tight liquid seal, (d) perfused ~ 20 μ L of cell suspension (10^6 cells/mL) for each cell type through a microchannel of the CFM (cells from the suspension saturate the surface after 10 min of gravitational settling), (e) contact of the CFM was maintained with the bottom of the well for 2–3 h while the apparatus was placed in a CO₂ incubator and the cell suspension allowed to adhere to the tissue culture treated well bottom, (f) washed the microchannels with ~ 0.25 μ L of medium to rinse away unadhered cells from the channels and filled the channels with air in order to relieve positive pressure of fluids in the deposition chamber, (g) added 200 μ L of medium to the well bottom in order to keep cells moist after removal of the CFM, (h) lifted the CFM from the well using the micromanipulator thumb screw leaving a set of cell microspots on the bottom of the well. The total time interval for steps (d)–(h) was ~ 3 h. To pattern cells using these processes the inlet and outlet channels designed into the CFM were necessary to infuse cells and culture medium

(steps (a), (c) and (d)), due to the tight seal of the CFM tip with the well bottom. The inlet and outlet channel system was also necessary for subsequent wash steps (step (f)). The deposition chamber was cut to a depth of 200 μ m at the tip of the *Y* interface between the inlet and outlet channels. This depth facilitated a gravitational settling time of 10 min as described in step (d). This depth also created sufficient stagnation within the region of cell adhesion at the well surface, so that adhered cells would not be washed away in step (f). The positions of each cell spot relative to the alignment marks were recorded just prior to step (h) by inspection through an inverted microscope. These positions are referred to for tracking the spots over the subsequent experiment steps. Spots that did not have a 10:1 signal to background cell count were excluded from the experiment as described below in the microscopy methods.

Dose-survival determination, microscopy and staining At 24 h after depositing and patterning the cells, the DNA of cells with compromised membranes were labeled by adding 1 μ M Sytox Orange dye (Molecular Probes, Eugene Oregon) in 500 μ L of new medium to each well for 30 min. The fluorescent labeling and transmitted light at each cell spot was imaged at its centroid using an Olympus LUCPlanFLN 20 \times (NA=0.45) objective lens on an Olympus IX70 inverted microscope (Olympus, Japan) equipped with a Optronics Microfire monochrome CCD camera (Optronics, California). Excitation of the dyes was provided by an Hg-arc lamp (Olympus, Japan). Sytox labeled cells were exposed for 300–600 ms (depending on the fluorescent level of dead floating cells) using U-MNG TRITC fluorescence filter cube providing excitation between 530–550 nm and transmitting to the camera at 590 nm. After Sytox labeling cells were washed with medium and 1 mL of new medium supplemented with 1% dimethyl-sulfoxide (DMSO) and a dose of mitomycin C (0, 0.1, 1, 10 μ g/mL) was added to each well.

Twenty-four hours after exposure to mitomycin C (48 h after patterning cells), the cells were washed with new medium, labeled and imaged immediately providing for a 24 h exposure to mitomycin C doses. The cells were then labeled with 160 μ M Hoechst 33258 cytoplasmic stain (Molecular Probes) in addition to Sytox Orange labeling. Hoechst labeled cells were exposed for ~ 7 ms using a U-MF2 DAPI fluorescence filter cube providing excitation between 360–370 nm and transmitting to the camera at 420 nm. Hoechst labeling was used to visualize cells and microspots at the end point and was not used in scoring live/dead cells.

The number of live cells in each microspot 24 and 48 h after cell patterning (post mitomycin C exposure) were scored by hand counting cells visualized in a 300 μ m \times 400 μ m field of view. The size of the cellular microspots was 200 μ m \times 300 μ m, so the field of view exceeded the

size of the microspots by 100 μm in both dimensions, making a single image sufficient for viewing the entire microspot and counting cells. Cells that fell outside of the imaging area were excluded from the count in order to reduce background noise. Examples of these images used to count cells are shown in Fig. 4(a), (b) and (c). These $20\times$ visible light and TRITC images taken at the centroid of the cell spots and the total number of live cells was determined by subtracting the number of Sytox labeled cells from the number of cells counted by visible light. Cells in the pre-marked background region were counted using a single field of view in the same fashion as the cellular microspots. The background image was taken with the same field of view ($300\ \mu\text{m}\times 400\ \mu\text{m}$) as the cellular microspots and all cells found inside this field of view were included in the background count. All cell spots that did not contain ten times the number of live cells as counted in the background region (signal to background of 10:1) immediately after patterning and 24 h after patterning were excluded from the experiment.

Statistical data analysis In order to test for statistically significant differences among the responses of the UV20 phenotype to the other CHO phenotypes (AA8, EM9, XRS-6) to equal doses of mitomycin C, independent two-sample one-tail Student *t*-tests with unequal sample sizes and unequal variances were used. To contrast each of the phenotypes with the UV20 phenotype three *t*-tests at each dose interval were conducted. One tailed *t*-tests (alternative hypothesis: UV20 mean < mean of other CHO phenotypes) were chosen because results of previous research have shown the expected hypersensitivity of UV20 to mitomycin C. *P* values <0.05 were taken to be statistically significant ($\alpha=0.05$). A correction for the α level was not made for multiple *t*-tests because these experiments were an exploration of the functionality of the device and intended to show that the device can produce data trending toward that produced by traditional techniques, even with small sample sizes. Exact *P* values have been reported for researchers wanting to use other statistical criteria. Results are reported as means \pm SD. All means were calculated with $n\geq 3$ sample size.

Chemicals and proteins XRS-6 CHO cells were obtained from Cambridge University (Cambridge, United Kingdom), the EM9, UV20 and AA8 CHO cells were obtained from American Type Cell Culture (Manassas, VA), α -MEM was obtained from HyClone, (Logan, UT), FBS from Summit (Ft Collins, CO), Fungisome from Biowhittaker (Walkersville MD), streptomycin and penicillin from Hyclone, trypsin/EDTA from GIBCO. The Hoescht and Sytox Orange fluorescent dyes were obtained from Molecular Probes (Eugene, OR) and mitomycin C from Sigma (St. Louis,

MO). The PDMS Sylgard 184 prepolymer was from Dow Corning (Midland, MI), SU-8 50 photoresist from Microchem (Newton, MA) and silicon wafers were from Silicon Quest International (Santa Clara, CA).

3 Results and discussion

Fabrication of the microfluidic deposition device With the fabrication techniques described, we developed a CFM with 200 μm high channels, cell deposition chambers of $200\times 300\ \mu\text{m}$ substrate contact area, 400 μm inter-deposition chamber spacing and 400 μm inter-row spacing. These size parameters can be further optimized for intended microspot sizes and inter-spot distances. The researcher may find that optimizing inter-spot distances is beneficial for cell–cell interaction studies (Folch and Toner 1998; Flaim et al. 2005) or that optimizing the viability and growth of a particular cell line is dependent on microspot size and cell packing density. The fabrication techniques presented here are intended to be flexible enough to develop the CFM to meet a variety of research needs.

Cell patterning We have tested the CFM for patterning up to four cell types simultaneously in a single well. In principle the CFM could pattern as many cell types as there are paired microchannels and the primary challenge with patterning a great number of cell types is related to the timely preparation of many cell suspensions.

Figure 2(a) shows the cells as seen before removal of the CFM (step (h)), the PDMS surrounding the deposition chamber shows up bright white due to the optical properties of PDMS (Chang-yen et al. 2006). An isolated spot of ~ 36 cells was left adhered to well bottom after removal of the CFM from the well (Fig. 2(b)). Figure 2(c) shows a set of four cell microspots and a region dedicated for background measurement; alignment marks are seen adjacent to the lower right hand corner of the spots.

Although the cytotoxicity experiments conducted only required that the cells remain healthy and viable for a 48 h period after the deposition, we studied the viability of cells patterned using the processes described for 111 h to show the viability of cells deposited using the CFM. CHO cell growth of eight $200\ \mu\text{m}\times 300\ \mu\text{m}$ microspots was observed over a period of 111 h (Fig. 3). During these 111 h cells were observed dividing (23 h doubling time), the microspots were observed expanding radially and the experiment was ended shortly before the adjacent microspots merged. The number of cells was measured by counting the total number of attached cells in the field of view of a $\times 20$ lens (as described in methods, but no staining exclusion was used). Eight microspots of cells were deposited, but only seven were tracked due to a failure of one spot to deposit

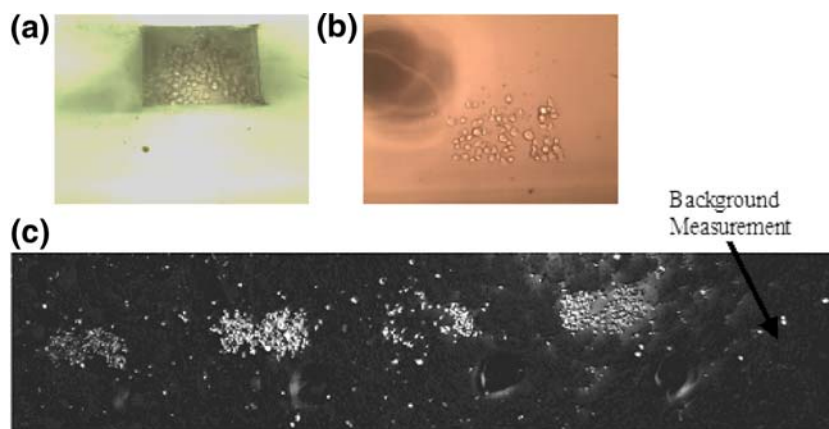


Fig. 2 Micropatterning cells in a tissue culture well using the CFM. (a) Cells incubating on the bottom of a tissue culture well while confined to the deposition chamber of the CFM. (b) Cells attached in a microspot on the collagen surface of the well after removal of the CFM. (Alignment mark visible in upper left) (c). Pattern of microspots

properly, providing a measure of microspot deposition yield (88%).

The uniformity of microspot density and viability (Table 1) was measured for 40 microspots 24 h after cell patterning. This data shows the process to produce a mean of 100 live cells per microspot 24 h after the deposition with a mean background of only three live cells. In an effort to determine the cause of the variance observed between microspots we conducted a test for randomness using the chi-squared comparison test of a distribution of microspots and the Poisson distribution. We found that microspots patterned with the same cell suspension at the same time tended to fit the random Poisson distribution while microspots patterned with the same cell suspension at separate times did not fit the Poisson distribution ($P < 0.05$, $n = 7$,

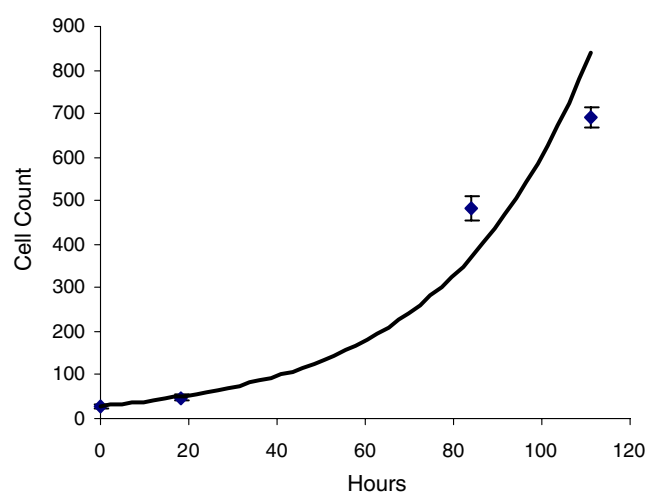


Fig. 3 Growth of CHO AA8 cells deposited into seven ($n = 7$) $200 \times 300 \mu\text{m}$ microspots. A doubling time of 23 h was calculated by using least squares linear regression ($r^2 = 0.986$) to fit the exponential growth curve shown ($\text{cells} = e^{0.030(t)}$)

of CHO cells (from left to right EM9, AA8, UV20, EM9) imaged 24 h after patterning. The background measurement region is marked on the right side of the array. (Alignment marks are visible to the lower right of each microspot and background measurement region)

$\chi^2 = 14$). This result lead us to conclude that a biological effect such as cell cycle contributes to the rate of cell adhesion leading to differences in microspot density.

It is also noteworthy that the restriction of a 10:1 signal to background (as described in Section 2) immediately after patterning and 24 h after patterning prevented cross-talk and guaranteed the ability to track spot positions. The use of a predetermined region for counting background cells in every experiment, may lead one to wonder if background may become an issue somewhere else in the well even when background cells fail to invade the background measurement area, but from our experience, all modes of background increase were readily detected in the background measurement area. A stringent wash of loose cells from the microchannels played a critical role in background reduction. Maintaining a leak-free system was also vital to a clean background. Overall, the PDMS seal at the spotter-substrate interface was quite good, and few leaks occurred contributing to a high microspot deposition yield.

Experiments revealed that monolayers of cells adhered to the well bottom of the deposition chamber for > 1.5 h were able to withstand pumping fluids through the microchannels. Tests using incremental increases in flow rate showed that cell adhesion was not compromised for flow speeds < 6 mL/h. This result indicates the ability of the CFM to deliver reagents to the cells during or following the

Table 1 Number of live cells counted in 40 microspots and nine background regions

	Mean no. of live cells	SE	Min	Max	Samples
Cell microspots	100	16	0	457	40
Background regions	3	1	0	9	9

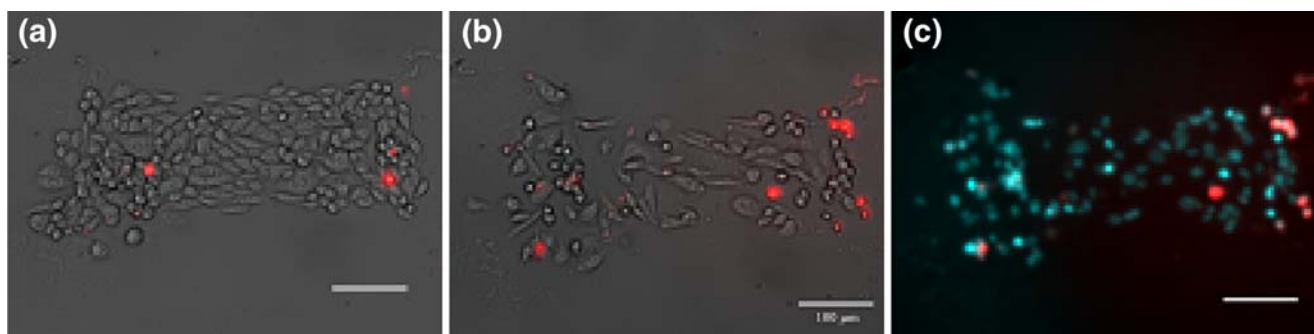


Fig. 4 Cell imaging process for a single microspot of EM9 cells dosed with 100 ng/mL of mitomycin C. **(a)** 20× Phase contrast and TRITC image overlay of microspot (cells with compromised membranes sytox labeled red) as seen 24 h after patterning. **(b)** 20× Phase

contrast and TRITC image overlay of microspot seen in **(a)**. after 24 h of incubation with 100 ng/mL of mitomycin C (48 h after patterning). The cell density has significantly diminished. **(c)** 20× DAPI and TRITC image overlay of the same microspot seen in **(b)**

deposition process. Because the CFM is also capable of depositing proteins and other biomolecules to the individual microspots of the array we foresee capabilities of the 48 microspot CFM to multiplex 48 cell types with 48 chemical reagents all within the confines of a 60 mm² area.

Dose survival determination In order to demonstrate usage of positive and/or negative controls and a parallel experimentation technique, two to four mutant cell types were patterned in each well (except for a few cases where the signal to background was <10:1 for part of the array) for dose survival experiments. Percent survival of cells from mitomycin C doses was determined by Eq. 1 (where the method of scoring cells is described in Section 2). Figure 4 demonstrates the measurements of cell viability from 24 h after cell patterning (Fig. 4(a)) to 48 h after cell patterning with 24 h of mitomycin C exposure (Fig. 4(b)) where the number of cells is visualized in phase contrast and dead Sytox labeled (Red) cells were excluded from the count. The experimental endpoint of the microspot is visualized with Hoescht (Blue) and Sytox (Red) labeled cells (Fig. 4(c)) 48 h after cell patterning. Figure 4(a) and (b) shows a reduction in cell density within the imaging region from 24 h post cell patterning to 48 h post cell patterning (after 24 h of exposure to mytomycin C) due to the detachment of dead cells from the well bottom. Increases in mitomycin dose lead to decreased microspot cell density along with an increase in the number of Sytox labeled cells indicating lower survival ratios for increased doses (Fig. 5(a)–(c)). Each data point in Fig. 5(a)–(c) was calculated by scoring the percent survival (Eq. 1) of three or more microspots ($n \geq 3$) each containing the same particular cell type and each interrogated at the same specific dose of mitomycin C. For an experiment of cell survival at a specific dose of mitomycin C. The microspots used in this average were patterned into a five spot arrays as described previously, and each array contained from two to four cell types. The combination of cell types used for each array varied from

experiment to experiment depending on which cell types were available for that day's experiment. Each array was interrogated with a specific dose of mitomycin C. These experiments were repeated by repatterning, dosing and rescoring spots until three or more microspots of a particular cell type at a specific dosing had undergone the experiment.

Several other morphological changes in cells were observed in cells with increasing doses, including; cell atrophy, grainy appearance, and roundness.

$$\% \text{ Survival} = \frac{\text{Viable cells 24 h after deposition}}{\text{Viable cells after 24 h of drug interrogation}} \quad (1)$$

The restriction of a 10:1 signal to background (as described in Section 2) had two purposes, to prevent cross-talk (as described earlier) and to prevent dead cells from entering the cytotoxicity experiment. One can easily judge from inspection of Fig. 4 that a large number of dead cells appearing on 24 h after cell patterning would be the contribution of earlier process steps and should be eliminated from the measurement of further induced responses in the microspot.

Phenotypic cytotoxicity determination For the micropatterned cell data of mitomycin C dose-survival ($n=54$), Two Way Analysis of Variance (ANOVA) testing ($\alpha=0.05$) followed by the Tukey Post-Hoc test showed highly significant ($P < 0.001$) dependence of cell survival on mitomycin C dose level over the entire set of CHO lines.

Results of the dose survival measurements of the micropatterned CHO phenotypes are shown in Fig. 5(a)–(c) and show the hypersensitivity of the UV20 cell line to the DNA interstrand cross-linking agent (mitomycin C). The trends of this parallel study observed in Fig. 5(a)–(c) show UV20 cells to have a reduced mean percent survival ($n \geq 3$) over two full log steps as compared to the other three cell types. In order to determine statistical significance ($P \leq 0.05$) among the differences in these small sample means we have used the Student *t*-test (Table 2). *t*-test comparison

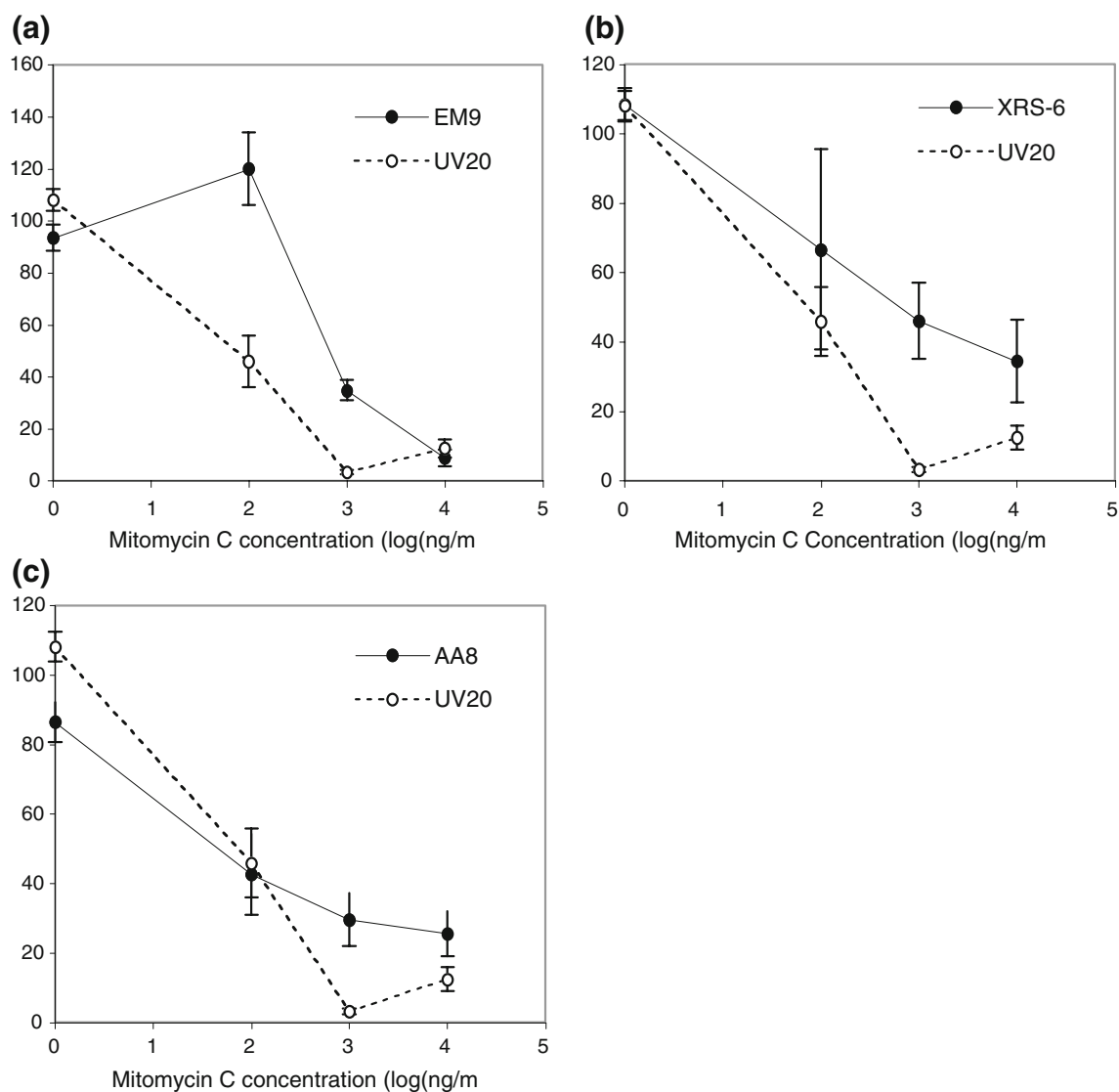


Fig. 5 Mean survival ($n \geq 3$) of microspots with increasing concentrations of mitomycin C. **(a)** Comparison of the UV20 positive control plotted with the CHO EM9 mutant. **(b)** Comparison of the UV20

positive control plotted with the CHO XRS-6 mutant. **(c)** Comparison of the UV20 positive control plotted with the CHO AA8 WT

Table 2 Significance table for the hypothesis $H_0: U_1 - U_2 = 0$ $H_1: U_1(U_2, \alpha = 0.05$, where U_1 and U_2 are the mean percent survival of the UV20 and compared CHO subtype, respectively, at the given dose level

CHO type	t statistic	One-tail test		Two-tail test		U2	SD	Sample
		P	t critical	P	t critical			
Mitomycin dose=0.1 $\mu\text{g/mL}$ $U_1 + \text{SD} = 46 + 42$ $n = 4$								
AA8	0.11	0.46	2.02	0.91	2.57	43	35	3
EM9	-2.35	0.04	2.13	0.08	2.78	120	42.37	3
XRS	-0.38	0.36	2.35	0.73	3.18	67	87	3
Mitomycin dose=1 $\mu\text{g/mL}$ $U_1 + \text{SD} = 3.2 + 3$ $n = 4$								
AA8	-2.02	0.09	2.92	0.18	4.3	38	30	3
EM9	-4.55	0.02	2.92	0.05	4.3	35	12	3
XRS	-2.26	0.08	2.92	0.15	4.3	46	33	3

between the UV20 and EM9 mutants shows statistically significant differences in mean percent survival over two log steps of mitomycin C doses, 0.1 $\mu\text{g}/\text{mL}$ ($P \leq 0.04$) and 1 $\mu\text{g}/\text{mL}$ ($P \leq 0.02$). While significant mean differences were not calculated by rejection of the null hypothesis for the other cell types within a single dose level, the mean values at the 1 $\mu\text{g}/\text{mL}$ mitomycin C dosing showed the UV20 phenotype to have a lower percent survival than the XRS-6 and AA8 phenotypes within the margin of error (shown with error bars in Fig. 5(b)–(c)). Comparative sensitivity of the UV20 mutant was also observed in an MTT test.

As seen in this experiment the CHO UV20 mutant has been shown to display hypersensitivity to DNA cross-linking agents (Thompson et al. 1980). This effect is expected and is attributed to deficiency in the ERCC1 nuclease. The excision repair cross complementing gene (ERCC1) has a substantial role in nucleotide excision repair, as well as recombination repair of DNA interstrand cross-links (Gaillard and Wood 2001) and repair of UV radiation damage. In humans the ERCC1-XPF nuclease complex plays a central role in these repair activities. Humans with the disease xeroderma pigmentosum have cells that are deficient in ERCC1-XPF and display hypersensitivity to UV radiation, as well as displaying sensitivity to DNA cross-linking agents (Thompson et al. 1980).

Mutant CHO cells defective in DNA repair pathways are a useful tool for studying human genes that correct their DNA repair defect. Human genes that correct these DNA repair deficiencies can be studied by transfecting the human gene into the repair deficient CHO cell (Thompson et al. 1980; Caldecott et al. 1992). For example it has been shown through gene transfection that five ERCC genes (ERCC1–ERCC5) can correct DNA repair mechanisms of cell mutants displaying UV radiation hypersensitivity (Thompson et al. 1990). The techniques demonstrated here could be applied to a wide variety of cell culture assays requiring high throughput screens of chemicals targeting repair deficient cell lines as well as genes leading to resistance of these chemicals. Clearly, studies focused on cell–cell interactions could also use this technology. Such as, studying the cell–cell interactions involved in metastasis and angiogenesis (Stetler-Stevenson et al. 1993) could be conducted with micropatterns of tumor cell colonies next to colonies of vascular cells. Cell micropatterns could facilitate tracking migration of these colonies and effectively studying agents that deter malicious migrations.

4 Conclusions

This study has shown our ability to pattern cells into tissue culture wells (17 mm deep and 16 mm wide) using high

aspect ratio microfluidic channels. With these patterns of cells we have compared the chemical responses of CHO phenotypes in a parallel study. This parallel cytotoxicity test shows statistically significant ($P < 0.05$) hypersensitivity of the UV20 CHO mutant to mitomycin C. Further refinement of the techniques and equipment used to infuse fluids with the microchannels may help minimize the amount of cells and reagents used for creating each micropattern. We conclude that the 48 microspot CFM will be capable of patterning up to 48 cell types within the confines of a 60 mm^2 area of a tissue culture well bottom, facilitating the parallel study of these cells in a small uniform environment.

Acknowledgements Kate Marshall and Chris Pond are acknowledged for their respective support in cell culture and technical assistance.

Funding sources Support for this effort is provided by the National Science Foundation (NSF) through the IGERT Program at the University of Utah, Grant Number DGE 9987616.

References

- L.R. Barrows, J.A. Holden, M. Anderson, P. D'Arpa, *Mutat. Res.* **408**, 103 (1998)
- D.A. Bartholomeusz, R.W. Boutte, J.D. Andrade, J. *Microelectromech. Syst.* **14**, 1364 (2005). doi:10.1109/JMEMS.2005.859087
- R. Brem, J. Hall, *Nucleic Acids Res.* **33**, 2512–2520 (2005). doi:10.1093/nar/gki543
- K.W. Caldecott, J.D. Tucker, L.H. Thompson, *Nucleic Acids Res.* **20**, 4575 (1992). doi:10.1093/nar/20.17.4575
- D.A. Chang-yen, D. Myszka, B.K. Gale, *JMEMS* **15**, 1145 (2006)
- X. Cheng, Y. Wang, Y. Hanein, K.F. Bohringer, B.D. Ratner, J. *Biomed. Mater. Res. A* **70**, 159 (2004). doi:10.1002/jbm.a.30053
- D.T. Chiu, N.L. Jeon, S. Huang, R.S. Kane, C.J. Wargo, I.S. Choi et al., *Proc. Natl. Acad. Sci. U S A* **97**, 2408 (2000a). doi:10.1073/pnas.040562297
- D.T. Chiu, N.L. Jeon, S. Huang, R.S. Kane, C.J. Wargo, I.S. Choi et al., *Nat. Acad. Sci.* **97**, 2408 (2000b). doi:10.1073/pnas.040562297
- D. Cortez, Y. Wang, J. Qin, S.J. Elledge, *Science* **286**, 1162 (1999). doi:10.1126/science.286.5442.1162
- C.J. Flaim, S. Chien, S.N. Bhatia, *Nat. Methods* **2**, 119 (2005). doi:10.1038/nmeth736
- A. Folch, M. Toner, *Biotechnol. Prog.* **14**, 388 (1998). doi:10.1021/bp980037b
- P.L. Gaillard, R.D. Wood, *Nucleic Acids Res.* **29**, 872 (2001). doi:10.1093/nar/29.4.872
- M. Goto, T. Tsukahara, K. Sato, T. Kitamori, *Anal. Bioanal. Chem.* **390**, 817 (2007)
- L.M. Kemp, P.A. Jeggo, *Mutat. Res.* **166**, 255–263 (1986)
- M.Y. Lee, C.B. Park, J.S. Dordick, D.S. Clark, *Proc. Natl. Acad. Sci. U S A* **102**, 983 (2005). doi:10.1073/pnas.0406755102
- M.E. Moynahan, T.Y. Cui, M. Jasin, *Cancer Res.* **61**, 4842 (2001)
- W.G. Stetler-Stevenson, S. Aznavoorian, L.A. Liotta, *Annu. Rev. Cell Biol.* **9**, 541 (1993). doi:10.1146/annurev.cb.09.110193.002545

- K.Y. Suh, J. Seong, A. Khademhosseini, P.E. Laibinis, R.A. Langer, *Biomaterials* **25**, 557 (2004). doi:[10.1016/S0142-9612\(03\)00543-X](https://doi.org/10.1016/S0142-9612(03)00543-X)
- P. Taverna, H. Hwang, J.E. Schupp, T. Radivoyevitch, N.N. Session, G. Reddy et al., *Cancer Res.* **63**, 838 (2003)
- L.H. Thompson, J.S. Rubin, J.E. Cleaver, G.F. Whitmore, K. Brookman, *Somat. Cell Mol. Genet.* **6**, 391 (1980). doi:[10.1007/BF01542791](https://doi.org/10.1007/BF01542791)
- L.H. Thompson, K.W. Brookman, N.J. Jones, S.A. Allen, A.V. Carrano, *Mol. Cell. Biol.* **10**, 6160 (1990)
- A.K. Vogt, G. Wrobel, W. Meyer, W. Knoll, A. Offenhausser, *Biomaterials* **26**, 2549 (2005). doi:[10.1016/j.biomaterials.2004.07.031](https://doi.org/10.1016/j.biomaterials.2004.07.031)
- C.W. Xu, *Genome Res.* **12**, 482 (2002)
- M.N. Yousaf, B.T. Houseman, M. Mrksich, *Proc. Natl. Acad. Sci. U S A* **98**, 5992 (2001). doi:[10.1073/pnas.101112898](https://doi.org/10.1073/pnas.101112898)
- J. Ziauddin, D.M. Sabatini, *Nature* **411**, 107 (2001). doi:[10.1038/35075114](https://doi.org/10.1038/35075114)
- T. Zhou, L.F. Povirk, *Mutagenesis* **20**, 39 (2005)